Document made available under the Patent Cooperation Treaty (PCT)

International application number: PCT/US04/019695

International filing date: 18 June 2004 (18.06.2004)

Document type: Certified copy of priority document

Document details: Country/Office: US
Number: 60/479,687
Filing date: 19 June 2003 (19.06.2003)

Date of receipt at the International Bureau: 19 August 2004 (19.08.2004)

Remark: Priority document submitted or transmitted to the International Bureau in compliance with Rule 17.1(a) or (b)

BEST AVAILABLE COPY

World Intellectual Property Organization (WIPO) - Geneva, Switzerland
Organisation Mondiale de la Propriété Intellectuelle (OMPI) - Genève, Suisse

1209401

THE UNITED STATES OF AMERICA

TO ALL TO WHOM THESE PRESENTS SHALL COME:

UNITED STATES DEPARTMENT OF COMMERCE

United States Patent and Trademark Office

August 10, 2004

THIS IS TO CERTIFY THAT ANNEXED HERETO IS A TRUE COPY FROM THE RECORDS OF THE UNITED STATES PATENT AND TRADEMARK OFFICE OF THOSE PAPERS OF THE BELOW IDENTIFIED PATENT APPLICATION THAT MET THE REQUIREMENTS TO BE GRANTED A FILING DATE.

APPLICATION NUMBER: ***60/479,687***
FILING DATE: ***June 19, 2003***
RELATED PCT APPLICATION NUMBER: ***PCT/US04/19695***

Certified by

Jon W Dudas

Acting Under Secretary of Commerce
for Intellectual Property
and Acting Director of the U.S.
Patent and Trademark Office

06-20-03

60479687 PTO/SB/16 (10-01)

Approved for use through 10/31/2002. OMB 0651-0032
U.S. Patent and Trademark Office; U.S. DEPARTMENT OF COMMERCE

Under the Paperwork Reduction Act of 1995, no persons are required to respond to a collection of information unless it displays a valid OMB control number.

PROVISIONAL APPLICATION FOR PATENT COVER SHEET

This is a request for filing a PROVISIONAL APPLICATION FOR PATENT under 37 CFR 1.53(c).

Express Mail Label No.	EV 315398556 US

INVENTOR(S)

Given Name (first and middle [if any])	Family Name or Surname	Residence (City and either State or Foreign Country)
Jacques	VANIER	Notre Dame del ille Perot, Canada

☐ *Additional inventors are being named on the ______ separately numbered sheets attached hereto*

TITLE OF THE INVENTION (500 characters max)

Determining the frequency modulation index of a laser in a CPT frequency standard

Direct all correspondence to: **CORRESPONDENCE ADDRESS**

☑ Customer Number 000025247 → *Place Customer Number Bar Code Label here*

Type Customer Number here

OR

☑ Firm *or* Individual Name	Gordon E. Nelson				
Address	57 Central St., P.O. Box 782				
Address					
City	Rowley	State	MA	ZIP	01969
Country	US	Telephone	978-948-7632	Fax	866-723-0359

ENCLOSED APPLICATION PARTS *(check all that apply)*

☑ Specification *Number of Pages* 25

☐ Drawing(s) *Number of Sheets* ____

☐ Application Data Sheet. See 37 CFR 1.76

☐ CD(s), Number ____

☑ Other (specify) Return postcard

METHOD OF PAYMENT OF FILING FEES FOR THIS PROVISIONAL APPLICATION FOR PATENT

☑ Applicant claims small entity status. See 37 CFR 1.27.

☑ A check or money order is enclosed to cover the filing fees

☑ The Commissioner is hereby authorized to charge filing fees or credit any overpayment to Deposit Account Number: 501315

☐ Payment by credit card. Form PTO-2038 is attached.

FILING FEE AMOUNT ($): $80.00

The invention was made by an agency of the United States Government or under a contract with an agency of the United States Government.

☑ No.

☐ Yes, the name of the U.S. Government agency and the Government contract number are: ____________

Respectfully submitted,

SIGNATURE Gordon E Nelson

Date 06/18/2003

TYPED or PRINTED NAME Gordon E. Nelson

REGISTRATION NO. *(if appropriate)* 30093

TELEPHONE 978-948-7632

Docket Number: kernco01.003

USE ONLY FOR FILING A PROVISIONAL APPLICATION FOR PATENT

This collection of information is required by 37 CFR 1.51. The information is used by the public to file (and by the PTO to process) a provisional application. Confidentiality is governed by 35 U.S.C. 122 and 37 CFR 1.14. This collection is estimated to take 8 hours to complete, including gathering, preparing, and submitting the complete provisional application to the PTO. Time will vary depending upon the individual case. Any comments on the amount of time you require to complete this form and/or suggestions for reducing this burden, should be sent to the Chief Information Officer, U.S. Patent and Trademark Office, U.S. Department of Commerce, Washington, D.C. 20231. DO NOT SEND FEES OR COMPLETED FORMS TO THIS ADDRESS. SEND TO: Box Provisional Application, Assistant Commissioner for Patents, Washington, D.C. 20231.

17522 U.S. PTO
17512 U.S. PTO 60/479687 06/19/03
EV315398556US

Contents of Provisional Patent Application for

Determining the frequency modulation index of a laser in a CPT frequency standard

Inventor: Jacques Vanier

A. Paper, *On the determination of the laser modulation index from the optical absorption spectrum for clock implementation by CPT*, 21pp.

B. Implementation supplement to A, 4pp.

6047968 7 .061903

A

Vanier-Kernco Nov 28-02
(Last edited Dec. 5, 2002)

On the determination of the laser modulation index from the optical absorption spectrum for clock implementation by CPT

Introduction

In the use of the CPT transmission absorption line for implementing a frequency standard, it is essential that the laser modulation index be set at a given value. In particular, it is interesting to set it at m = 2.4, the value that makes the power light shift equal to zero. In that case the clock frequency is essentially independent of laser power. It can also be set at about 2.6-2.8, where there is a minimum in the light shift curve against modulation index, making the clock frequency independent of the index in first order. Which setting is best regarding frequency stability is not yet known. Experiments will decide.

However, before adopting either approach, it is necessary to see if we can set easily the modulation index to a prescribed valuc without too much effort. In the standard method, a Fabry-Perot interferometer is used for that purpose. It is the first tool that comes to mind. However, the setting of the instrument and the measurement process is complex. Furthermore, it requires the laser to bc cxamined independently of the actual clock setup. An approach in which the laser modulation can be evaluated in situ without disassembling the clock should provide a net gain. Such an approach is possible through the direct examination of the light absorption spectrum at the exit of the cell by means of the same photodetector diode as that used in the detection system of the CPT transmission resonance line. This is what is examined in the present report.

The spectrum of the modulated laser is calculated at the exit of the Rb gas cell, as observed at the photodetector. The analysis is done as a function of the modulation index of the laser. The analysis is done also as a function of light intensity, Rb density and buffer gas pressure. The results are compared to the experimental data obtained in the laboratory. Conclusions are drawn on the feasibility of the technique.

The analysis does not take into account optical pumping taking place at high light intensity. However, since the theoretical results neglecting this effect are in good agreemcnt with the experimental data, it is concluded that the technique can be used in practice with reasonable accuracy.

A future report will discuss in more detail the effect of optical pumping and provide additional information on its influence in the implementation of the technique for adjusting the index of modulation.

It should be realized that the technique could be included directly in the start sequence of a frequency standard using the digital approach.

The setup

The standard CPT setup is shown in Fig.1.

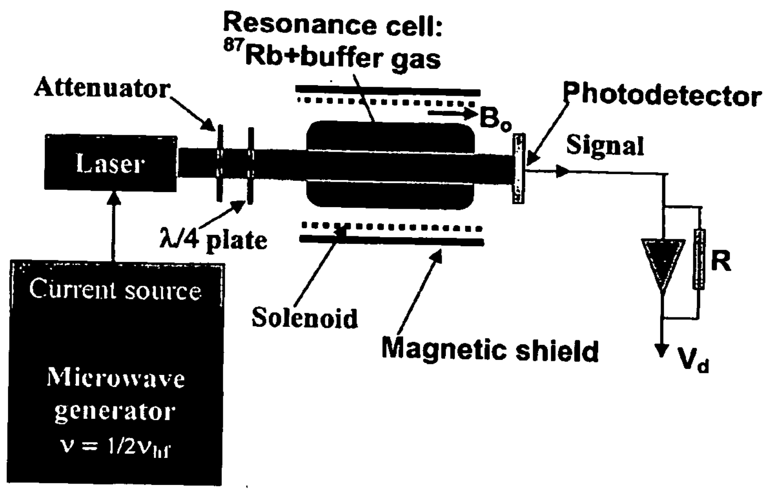

Figure 1. Experimental setup.

The output of the transimpedance amplifier is V_d proportional to the light intensity falling on the detector. V_d is a measure of the total light spectrum. There is no frequency discrimination in the detection process and the output voltage is the sum of all the laser sidebands after absorption by the cell.

The absorption spectrum.

The Rb atoms in the cell are characterized by the energy level structure shown in Fig. 2.

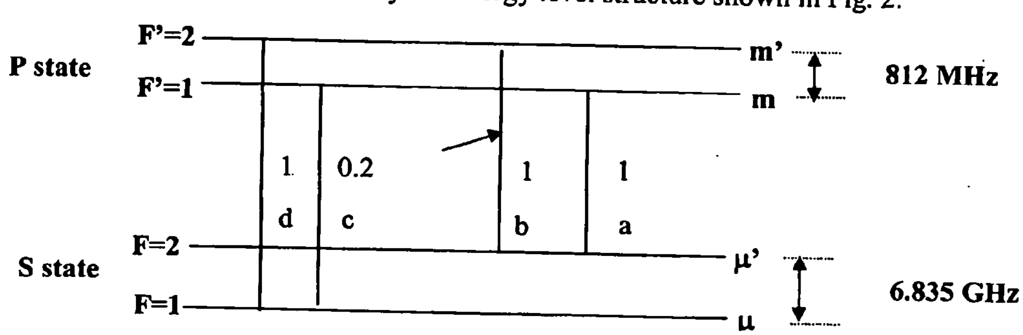

60479687 .061903

Figure 2. Illustration of the four hyperfine transitions of the D1 line of ^{87}Rb with their respective transition probability.

If the laser is monochromatic, not modulated, the cell acts as a frequency discriminator providing four absorption lines, a, b, c and d, easily identified by sweeping the laser frequency slowly over the spectrum. The width of these lines is of thc ordcr of 700 to 1000 MHz depending on the buffer gas pressure. The hyperfine lines are all resolved, although overlapping to a certain extent. A typical spectrum is shown in Fig. 3 with the respective lines identified. It is readily observed that line c has a much lower intensity than the others do, as predicted by the transition probability shown in figure 2.

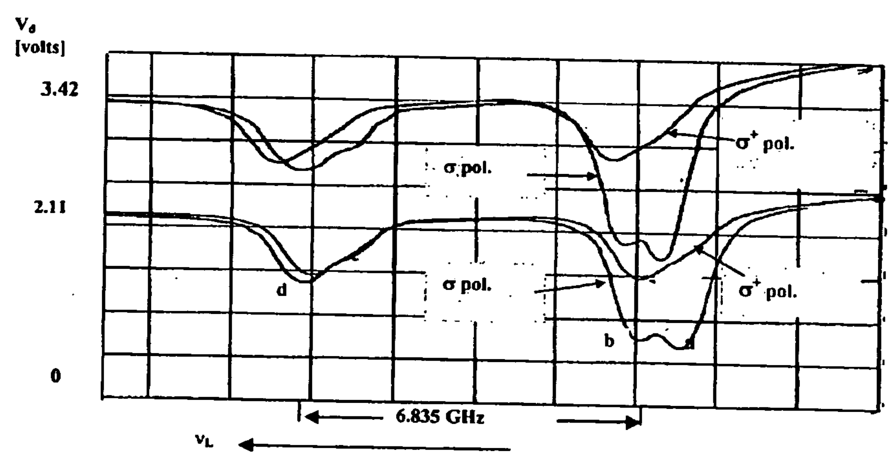

Figure 3 Typical absorption spectrum observed in ^{87}Rb in buffer gas.

It is observed that when circular polarization σ^+ or σ^- is used, there is reduction of the absorption of line a. The most likely explanation is optical pumping to a Zeeman level that is not in interaction with the laser radiation. The population of the absorbing level is reduced and the absorption involving that level is also reduced. When the laser frequency is scanned across the absorption spectrum there is also optical pumping from one hyperfine level to the other hyperfine level. If the scan is slow as is normally the case, an equilibrium is reached where one ground state hyperfine level is more populated than the other, reducing the optical absorption. The first

process is present in the observation of the dark line because circularly polarized light is required for the observation of the 0-0 transition. The second process is not present to the same extent in the observation of the dark line since the two ground state hyperfine levels are equally pumped by the two radiation fields J_{1+} and J_{1-} of equal intensities. Experiments show, as expected, that optical pumping is more important at high light intensity.

These effects will be examined in more details in a future report and their consequence on the present analysis will be outlined.

Theoretical background

The radiation amplitude of the "n"th sideband in the laser spectrum is described by the electric field E_{on}. We define the Rabi frequency proportional to this electric field as :

$$\omega_{Rnij} = (E_{on}/\hbar) \langle i|er\bullet e_\lambda|j\rangle \qquad (1)$$

This definition is introduced in order to simplify notation and provide better insight into the physical mechanisms taking place in the laser radiation absorption process. In that equation, n is the sideband identification, $\hbar$ is Planck's constant over 2π, and the terms between brackets represent the electric dipole matrix element characterizing the transition between levels i and j. It is generally written as d_{ij} and gives the intensity of absorption.

Absorption is described by the differential equation derived from the Maxwell's field equation coupling the radiation electric field to the polarization of the Rb ensemble. The polarization of the Rb ensemble is calculated in the density matrix formalism through solving the appropriate rate equations for the level populations and the coherence existing in the system and introduced by the laser radiation. For sideband n and transitions between levels i and j an exact calculation gives:

$$\frac{\partial \omega_{Rnij}}{\partial z} = \alpha_{ij} \operatorname{Im} \delta_{nij} \qquad (2)$$

where α is the absorption coefficient defined as

$$\alpha_{ij} = \left(\frac{\omega}{c\varepsilon_o \hbar} d_{ij}^2 \right) n_{Rb} \qquad (3)$$

All the effects of optical pumping and coherent population trapping are imbedded into the term $\operatorname{Im}\delta_{nij}$, which means imaginary part of the off diagonal density matrix element δ_{nij}. It is the optical coherence created in the system by the radiation field sideband E_n at the transition frequency coresponding to the transition between levels i and j. The transition probability for transition i to j is imbedded in the matrix dipole moment d_{ij}. On the other hand, the various terms in α_{ij} are defined as follows: ω is the average laser frequency, c is the speed of light, ε_o is the permittivity of free space and n_{Rb} if the Rb density.

If we neglect optical pumping from one level to another level of the ground state, $\operatorname{Im}\delta_{nij}$ is given by;

$$\operatorname{Im} \delta_{nij} = -\left(\frac{\omega_{Rnij} (\Gamma/4)}{(\Gamma/2)^2 + (\Omega_{nij})^2} \right)$$

(4)

where Ω_{nij} is

$$\Omega_{nij} = \omega_n - \omega_{ij} \tag{5}$$

ω_n being the laser sideband angular frequency and ω_{ij}, the angular frequency of thc atomic transition.

In the theory, parameter Γ is the decay rate from the excited state caused by Rb-buffer gas atom collisions. Unfortunately, there is always broadening from Doppler effect and in practice the absorption line width is larger than that expected just from the excited state decay rate. Actually the optical absorption line is a convolution of a Gaussian line shape (Doppler effect) and of a Lorentz line shape (decay from the excited state: Voigt profile). In that context the problem is intractable since the solution of the above differential equation would need to be integrated over all velocities. However, since in practice the line shape observed is closely Lorentzian, it is possible to approximate the situation by assuming a decay rate that gives an absorption line width the same as the one observed. This is the approach we use. In that case the differential equation can be integrated directly and gives Beer's law for absorption:

$$\omega_{Rn}(z) = \omega_{Rn}(0)\exp -\alpha_{ij}\left(\frac{(\Gamma/4)}{(\Gamma/2)^2 + (\Omega_{ijn})^2}\right)z \tag{6}$$

where Γ is now a pseudo-decay rate giving a line width $\Delta\nu_{opt}$ equal to $(1/2\pi)\Gamma$, approximating the measured line width.

In this expression $\omega_{Rn}(0)$ is the value of the Rabi frequency at the entrance of the cell. According to Eq. 1, it is proportional to the radiation electric field of the nth sideband. The voltage measured at the photodetector of the setup shown in Fig. 1 is proportional to the intensity of the radiation, thus to the square of the electric field of thc radiation. Furthermore this voltage is proportional to the sum of all the radiation fields traversing the absorption cell, that is all the sidebands. Consequently a summation must be made over all these sidebands n. Furthermore a summation must also be made as well on all the absorption lines <i|j> shown in Fig 2. The result is:

$$(\omega_R(z))^2 = \sum_n (\omega_{Rn}(0))^2 \exp -2\sum_{ij} a_{ij}\alpha\left(\frac{(\Gamma/4)}{(\Gamma/2)^2 + (\Omega_{ijn})^2}\right)z \tag{7}$$

We have also introduced the coefficient a_{ij} that takes into account the actual transition probability shown in Fig. 2 and leaves α as a general term constant for all transitions.

Since V_d is proportional to the square of the Rabi frequency this equation can be written as

$$V_d = k\sum_n (\omega_{Rn}(0))^2 \exp -2\sum_{ij} \alpha_{ij}\left(\frac{(\Gamma/4)}{(\Gamma/2)^2 + (\Omega_{ijn})^2}\right)z \tag{8}$$

Here k is a constant representing the transformation of light intensity (Rabi frequency) into voltage by the detection system.

Approximations made

In the analysis optical pumping was not included. The theoretical results obtained, however, are in fairly good agreement with the experimental observations. It appears that although optical pumping is present to some extent, it introduces only a small distortion of the absorption spectrum. It will be shown below, through the analysis of the experimental data at three light intensities, that this distortion is not a serious impediment to the use of the technique in fixing the modulation index. In practice the effect is smaller at low light intensity.

The constant to be used

The decay rate Γ: the physics behind this parameter was discussed above. In practicc it is set such as to give good agreement with the line width observed experimentally, assuming a Lorentz line shape. The value used hcre for a cell containing a N_2-Ar buffer gas mixture at 10 Torr is 4 x $10^9 s^{-1}$.

The absorption coefficient α : from a previous calculation on the contrast of the transmission CPT signal it was found that at 65 °C good agreement was obtained between theory and experimental data with a value of 2.1 x $10^{11} m^{-1} s^{-1}$. This is the value we will use.

Transition probability a_{ij}: It is taken as that given in Fig. 2. It is 1 for all transitions and 0.2 for the transition μ to m.

The value of the Rabi frequency at the entrance of the cell $\omega_{Rn}(0)$. We set it for the carrier, for an unmodulated laser. We assume a value equal to 2 x 10^6. The size for the various sidebands is then obtained through a multiplication by the appropriate Bessel function valuc for the index of modulation chosen.

The calculation.

The calculation is done in Mathematica software with the constant chosen above. An example of thc results of the absorption spectra obtained for an index of modulation equal to 1.8 is shown in Fig. 4. Detailed results are given in Annex I. Only the J_2, J_1 and J_o sidebands are used in the calculation.

m=1.8 w_R=Intensity of radiation transmitted W=Δfrequency

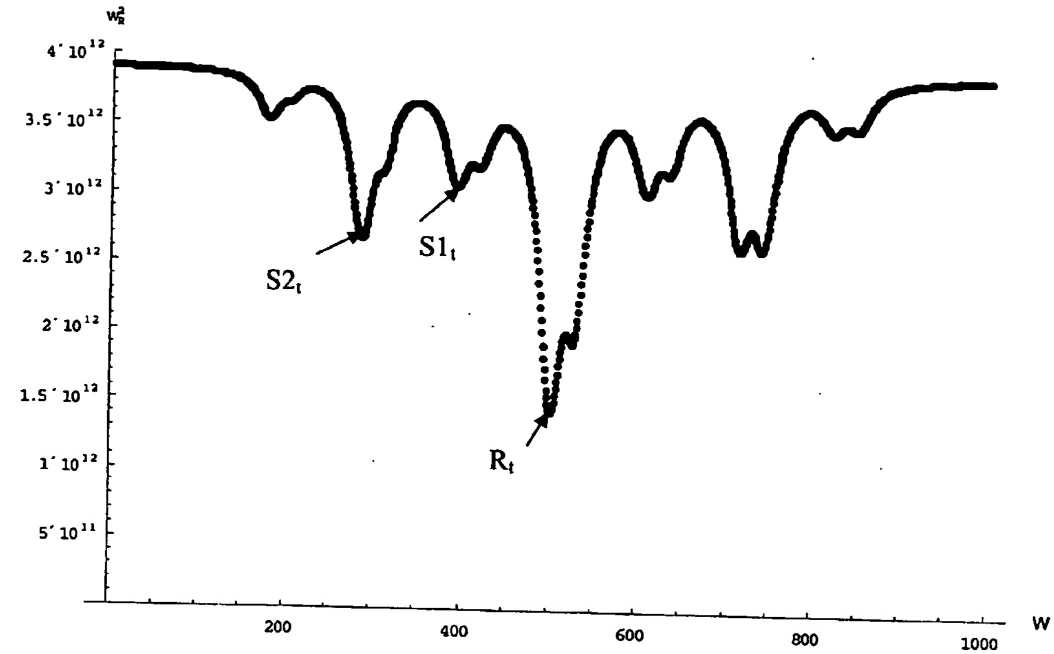

Figure 4 Theoretical absorption spectrum of 87Rb, D1 resonance optical line. The laser is assumed monochromatic and modulated with an index of 1.8. The constants used in the model are explained in the text.

Experimental results

A typical experimental result for a modulation index of ~1.5 is shown in Figure 5.

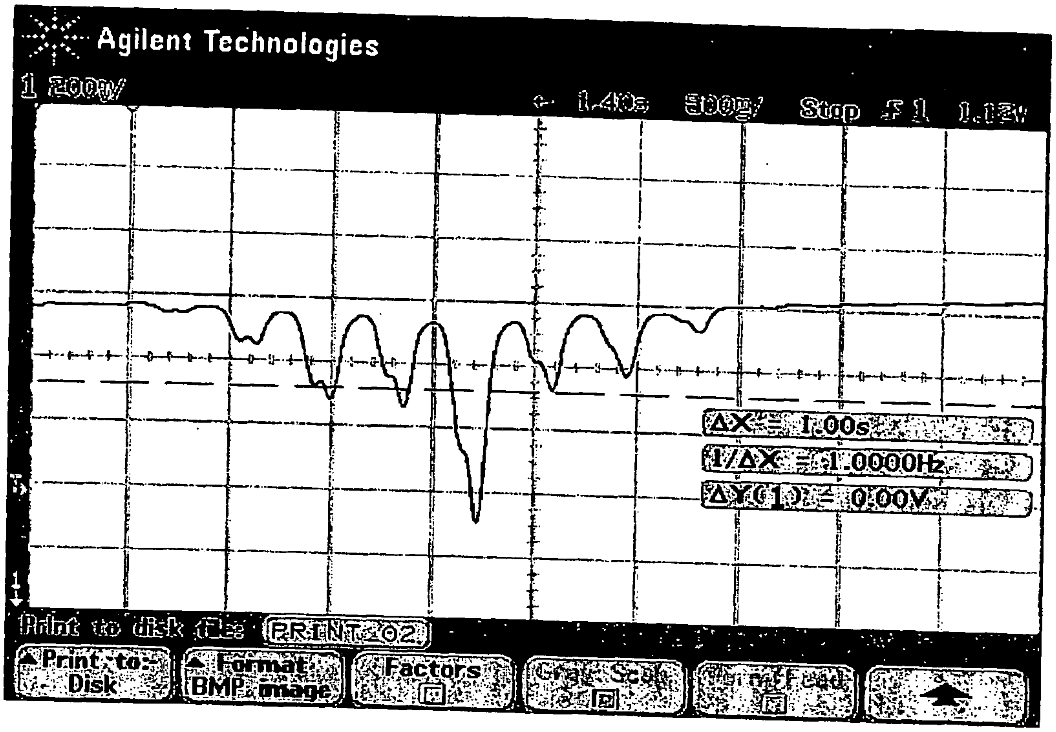

Figure 5. Experimental absorption spectrum in ^{87}Rb observed on an operating CPT Clock with a frequency modulated VCSEL.

It is readily observed from Annex I that there nearly exist a one to one correspondence between the theoretical and the experimental results reported in Figure 5. Visual observation is sufficient to evaluate the index of modulation to approximately 10 %.

Determination of the index of modulation

The index of modulation can readily be evaluated by plotting the ratios (R_t/ $S1_t$), and ($S1_t$/$S2_t$). These terms are defined in Fig 4. Due to the form of Eq. 7, these ratios are essentially ratios of Bessel functions included in the values of ω_{Rn}. These ratios are plotted for the theoretical results in Fig. 6. Experimental results for the three optical densities studied are plotted in Figures 7, 8 and 9.

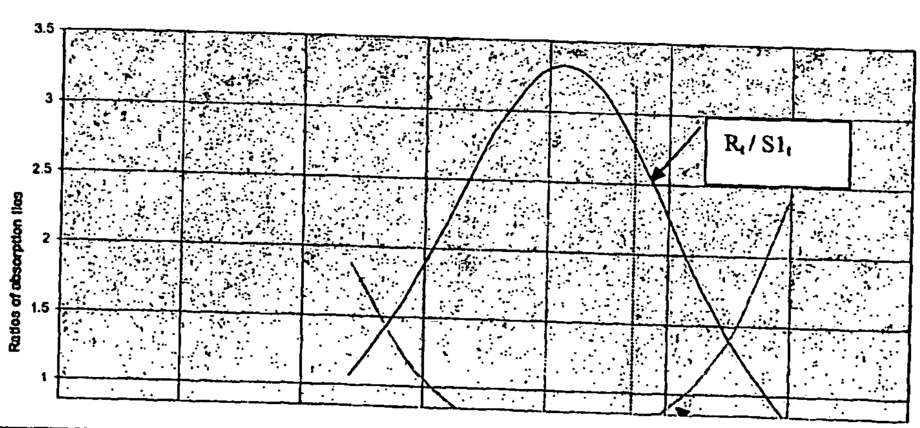

60479687 .061903

Figure 6. Theoretical ratio of resonance and satellite lines

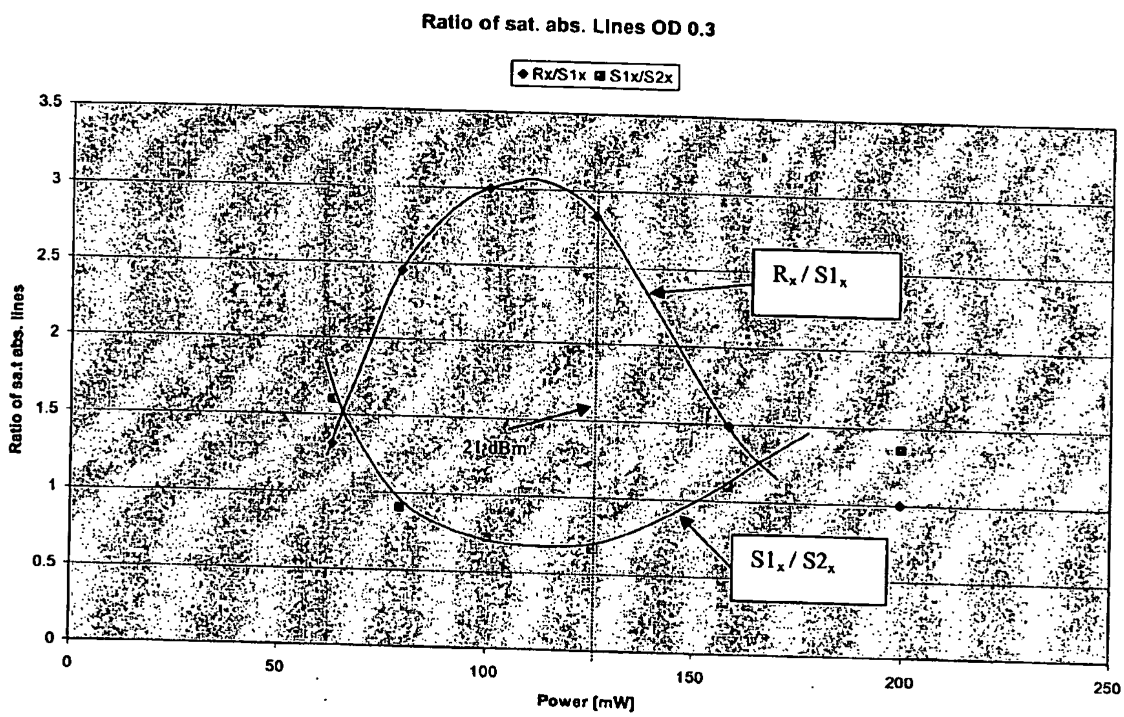

Figure 7 Experimental data on resonance and satellite ratios for light intensity corresponding to a gray filter with optical density equal to 0.3 placed in the path of the laser beam.

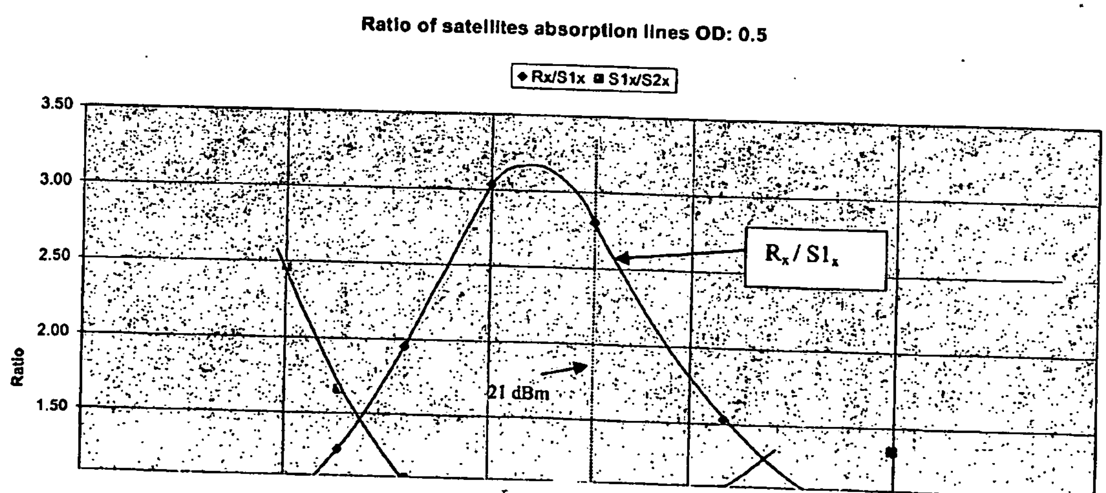

Figure 8. Experimental data on satellite ratios for light intensity corresponding to a gray filter with optical density equal to 0.5 placed in the path of the laser beam.

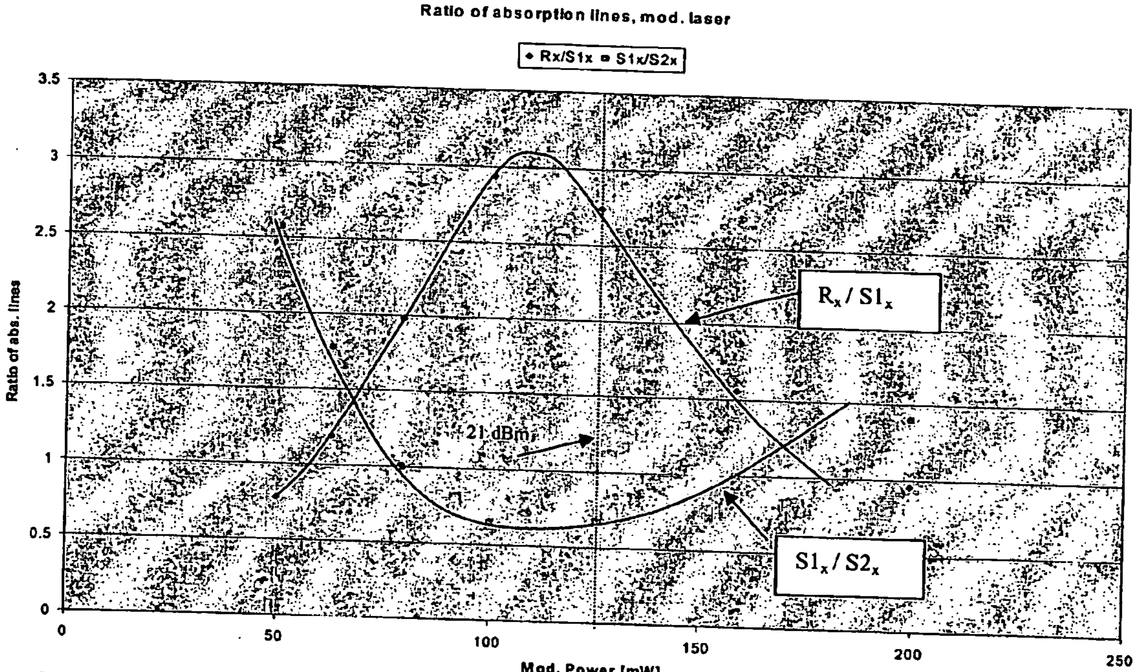

Figure 9. Experimental data on resonance and satellite ratios for light intensity corresponding to a gray filter with optical density equal to 0.8 placed in the path of the laser beam.

As is readily observed there is good correspondence between the experimental an theoretical graphs at moderate modulation power (< 150 mW) and it is possible to determine the index of modulation to better than 10% by simply measuring the ratio $R_x/S1_x$ or $S1_x/S2_x$. For example at 125 mW, 21 dBm, the index is about 2.4.

At higher power (>150mW), it appears that there is saturation in the system. It is not clear where this effect comes from. It is possible that the synthesizer is not linear with power above 150 mW.

Effect of optical pumping rate, line width and temperature.

The same calculation were done for three other situations in relation to the absorption coefficient (higher temperature, $T_{cell} = 75°C$), the Rabi frequency (doubling the light intensity) and the optical line width (increase by 50%).

The results are shown in Annex I. It is observed that when the light intensity is doubled the absorption spectrum shape does not change. Only the absolute value of the light transmitted is increased. This is expected since the light intensity does not alter the optical line width, and optical pumping has been neglected. It is also seen that values of Γ and α other than those used above in the calculation do not provide better agreement between experimental and theoretical data.

Conclusion

It appears that the theoretical results are in fairly good agreement with the experimental data.

1) Except for small differences in the low frequency absorption lines of the spectra (right hand side of recorded spectra) the shapes are rather similar and vary with index of modulation very much like the experimental data vary with microwave power. The small differences are believed to be due to Zeeman optical pumping taking place under circular polarization.

2) Differences between experimental data and theoretical data at high modulation power are believed to originate from non-linearity of the microwave generator. (This conclusion should be verified by appropriate calibration).

3) A visual examination of the theoretical and experimental spectra is sufficient to determine that the experimental case of 22 dBm corresponds to a modulation index m equal to 2.6, while 21 dBm corresponds rather closely to m = 2.4. Calculation of actual ratio of satellite amplitudes provides an effective mean of determining the modulation index better than the 10% obtained by visual inspection. The ambiguity that results from the quasi-parabolic response of these ratios, (same ratio of satellites for two different microwave powers or modulation index), can be removed by examination of the minimum or maximum of the ratios observed.

Annex I

Figure A1. Theoretical results: absorption spectrum of modulated laser radiation. Only the sidebands J_o, J_1 and J_2 are taken into account. J_3, if considered, would add a small component at the higher values of modulation index. The constant assumed are $\Gamma = 4 \times 10^9 s^{-1}$, $\alpha = 2.1 \times 10^{11} m^{-1} s^{-1}$ and $\omega_R = 2 \times 10^6 s^{-1}$. These corresponds to a typical situation: $T_{cell} = 65°C$,

P_{BG} =10 Torr, and a light intensity that produces and added dark line broadening of the order of 250 Hz.

Notation:

- Muv means an Index of modulation equal to (u.v). For example, m0 means that only the carrier is present while m16 means an index of modulation equal to1.6.

-The second figure (m12) identifies lines to be used in the analysis. R_t corresponds to the line used for dark line resonance observation, while $S1_t$ and $S2_t$ are satellites used in the determination of the index of modulation. Subscript t stands for theoretical x later used means experimental.

m=0 w_R=Intensity of radiation transmitted W=Δfrequency

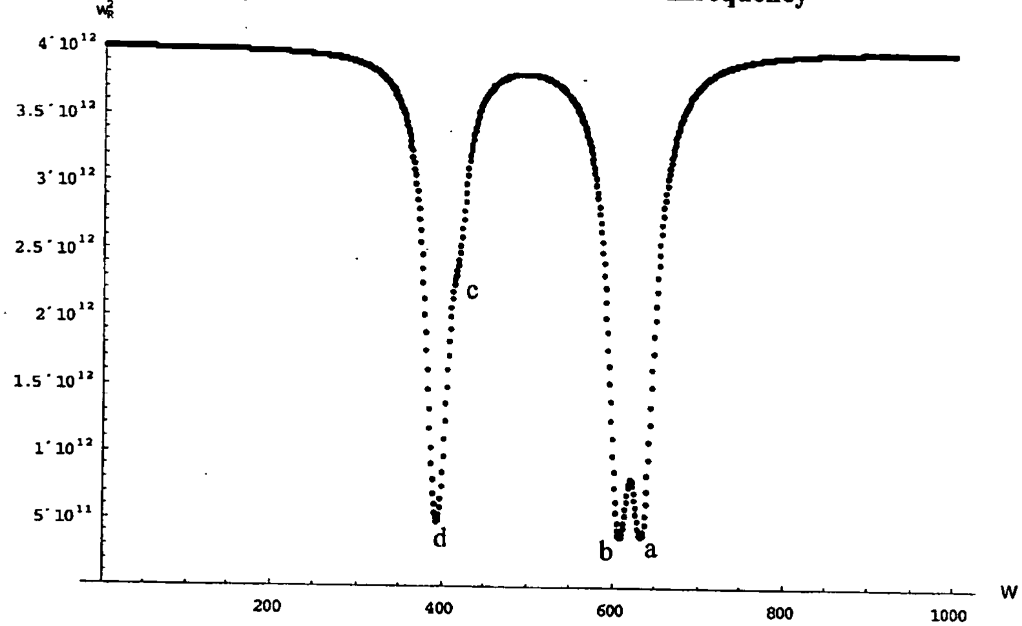

m=1.2 w_R=Intensity of radiation transmitted W=Δfrequency

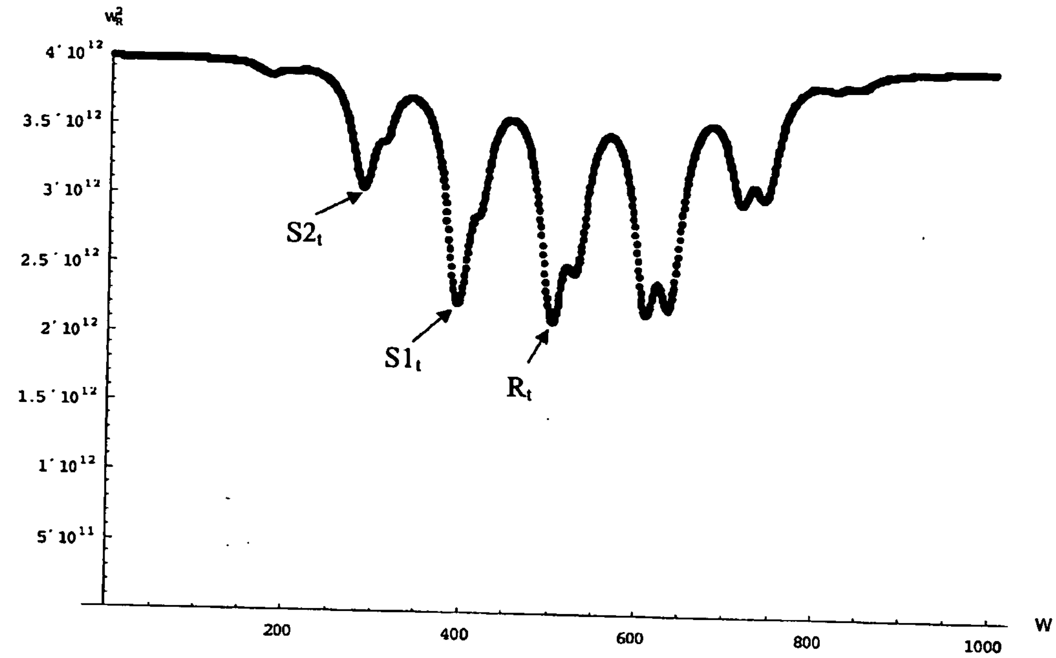

m=1.4 w_R=Intensity of radiation transmitted W=Δfrequency

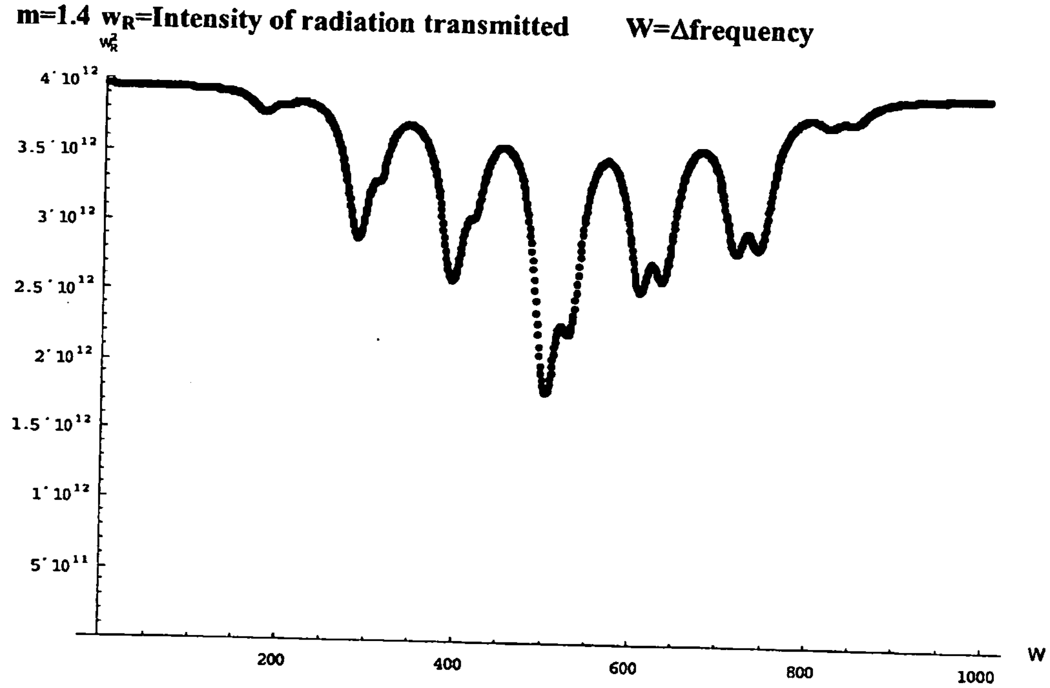

m=1.5 w_R=Intensity of radiation transmitted W=Δfrequency

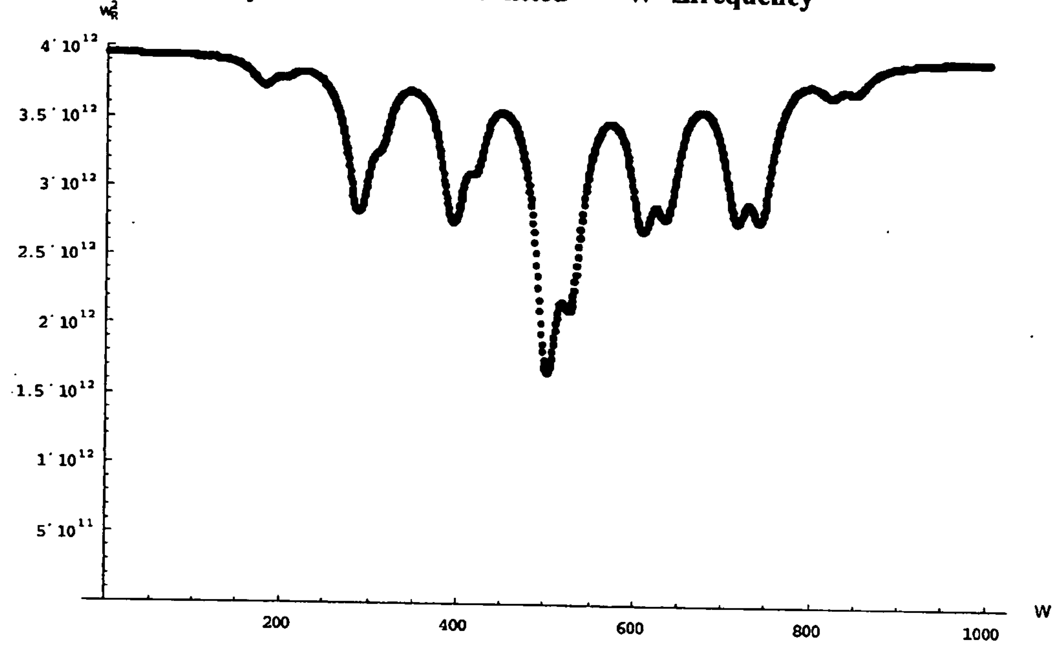

m=1.6 w_R=Intensity of radiation transmitted W=Δfrequency

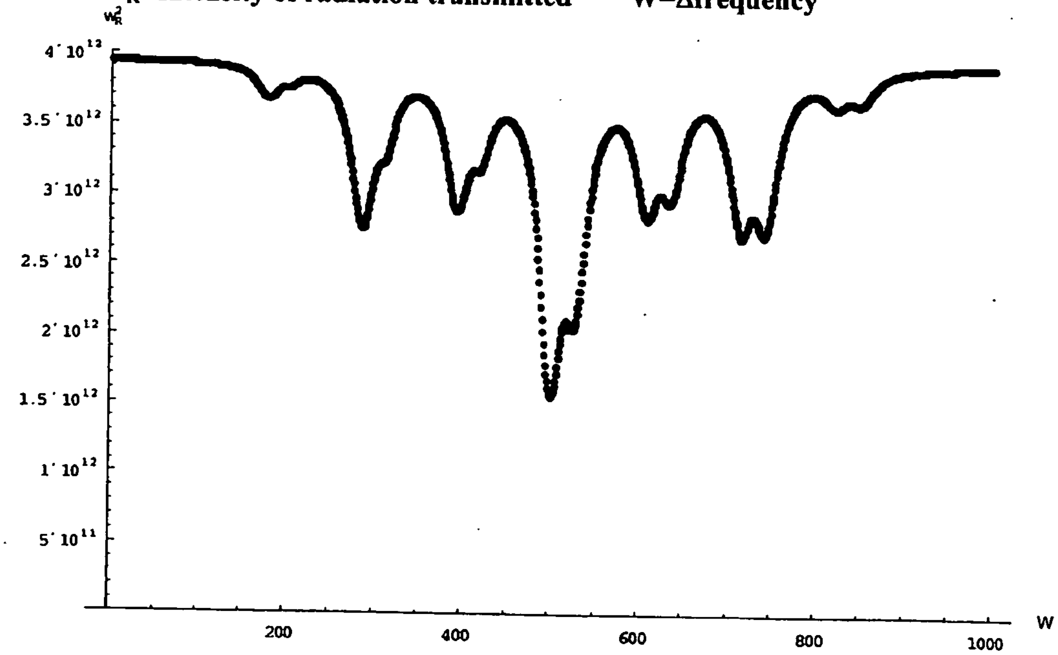

m=1.7 w_R=Intensity of radiation transmitted W=Δfrequency

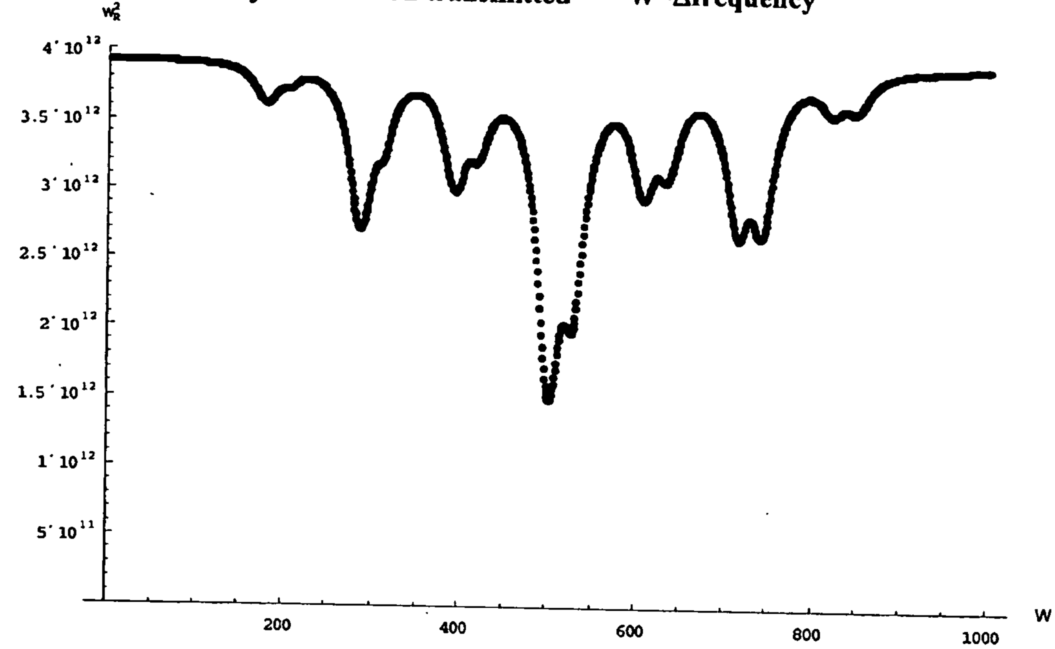

m=1.8 w_R=Intensity of radiation transmitted W=Δfrequency

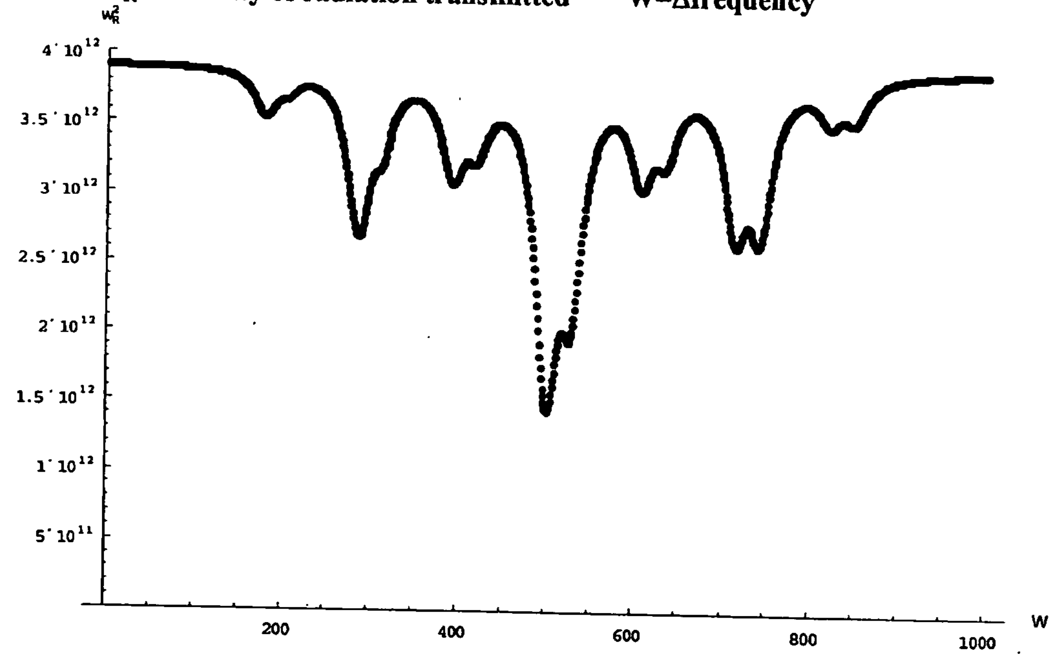

m=2.0 w_R=Intensity of radiation transmitted W=Δfrequency

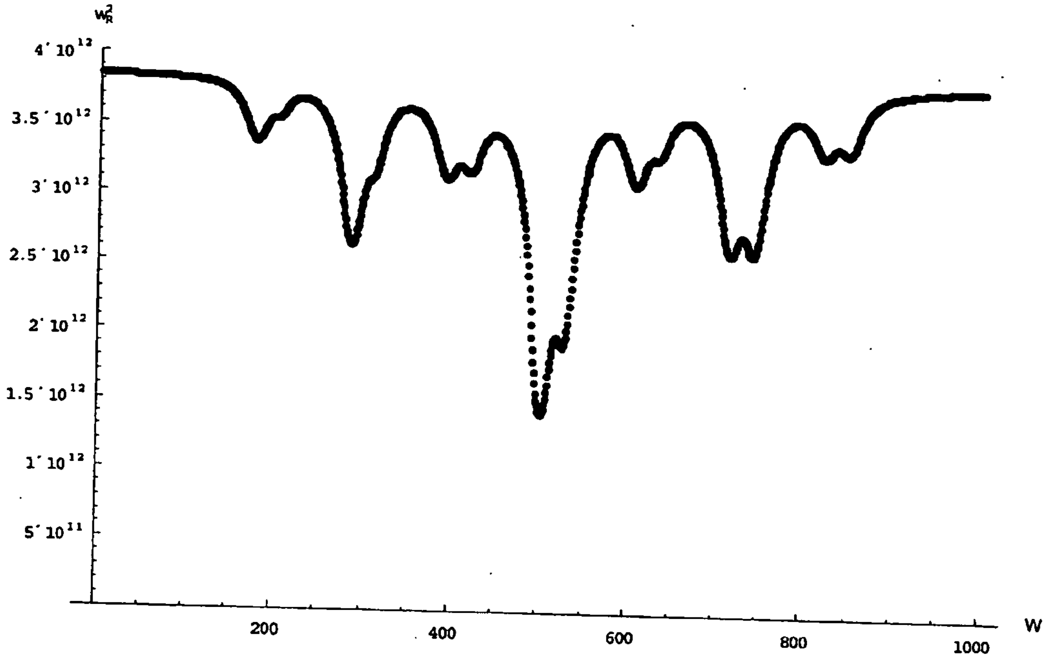

m=2.2 w_R=Intensity of radiation transmitted W=Δfrequency

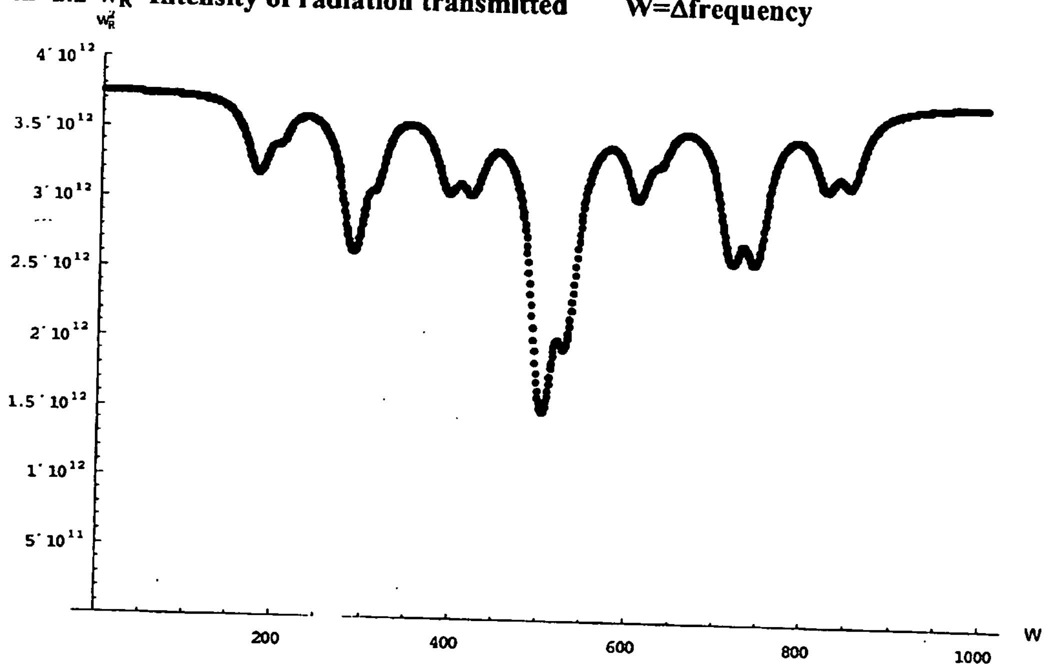

m=2.4 w_R=Intensity of radiation transmitted W=Δfrequency

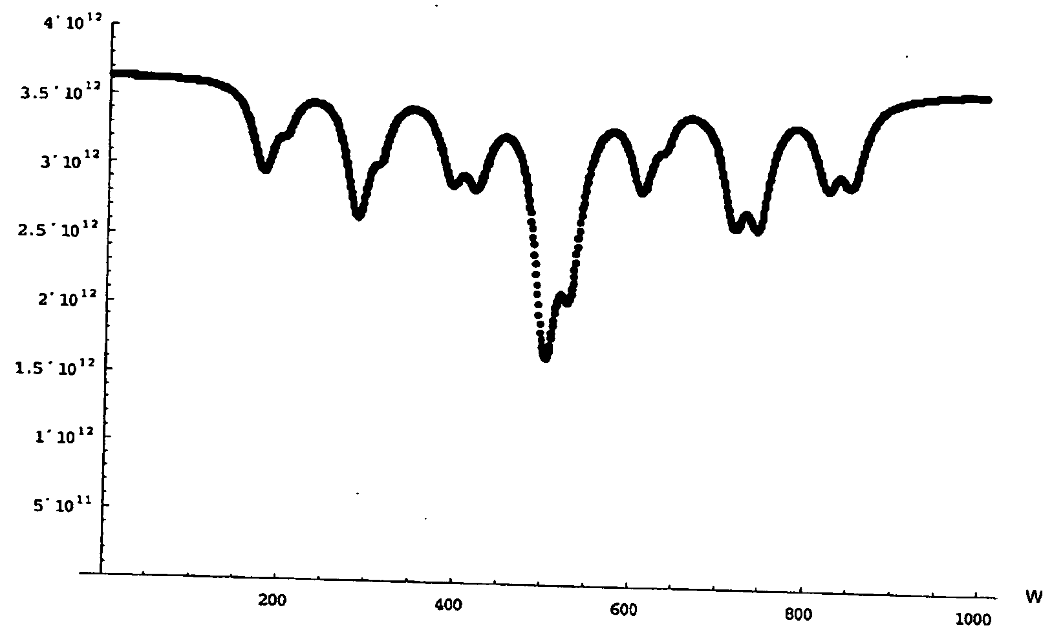

m=2.6 w_R=Intensity of radiation transmitted W=Δfrequency

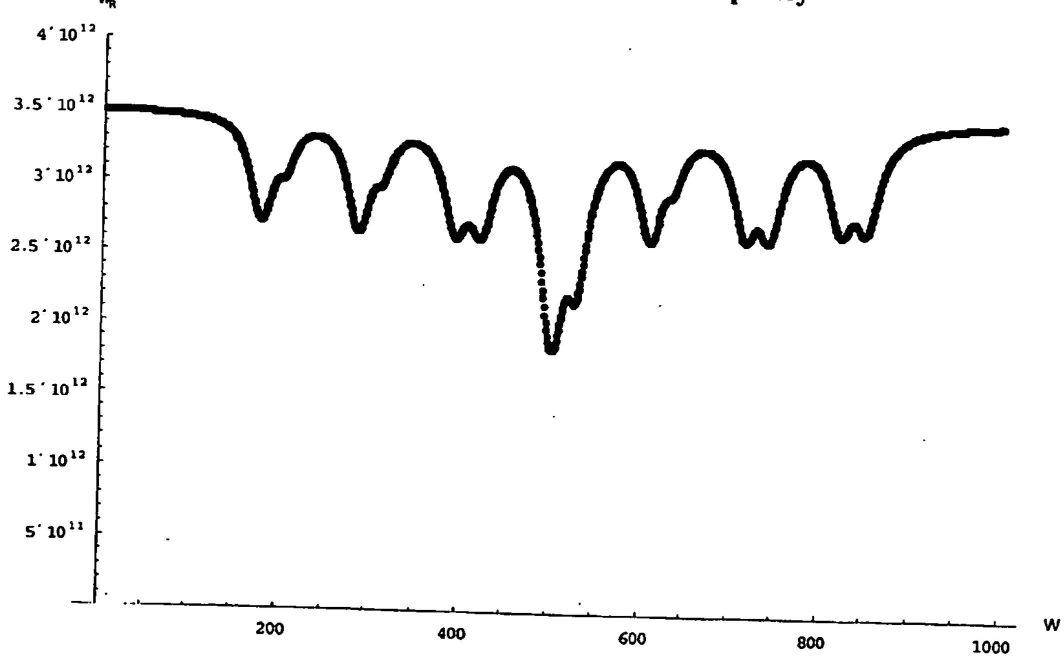

m=2.7 w_R=Intensity of radiation transmitted W=Δfrequency

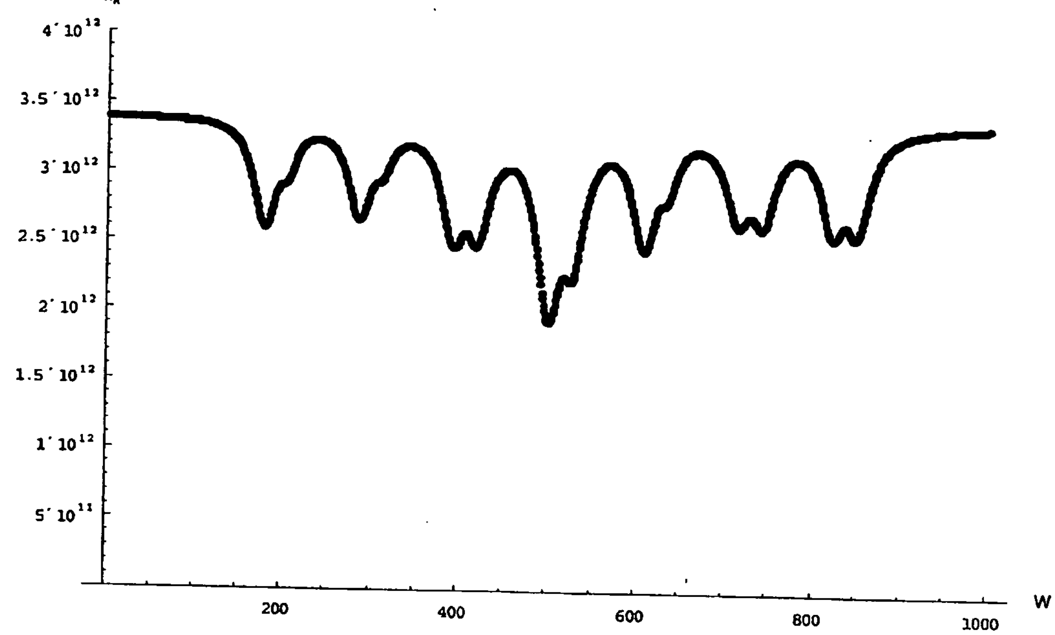

m=2.8 w_R=Intensity of radiation transmitted W=Δfrequency

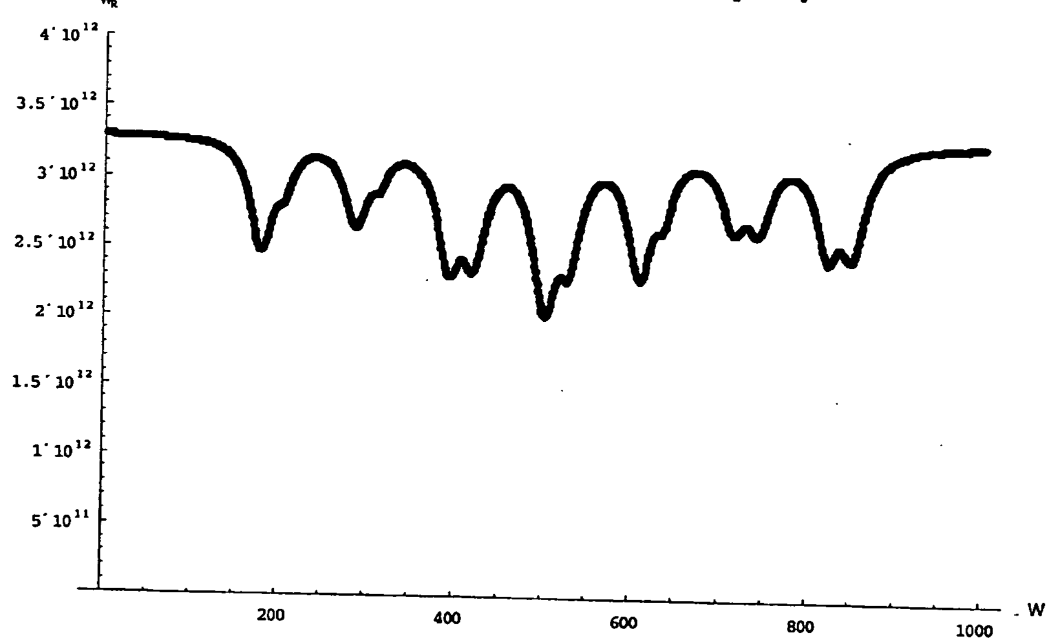

m=3.0 w_R=Intensity of radiation transmitted W=Δfrequency

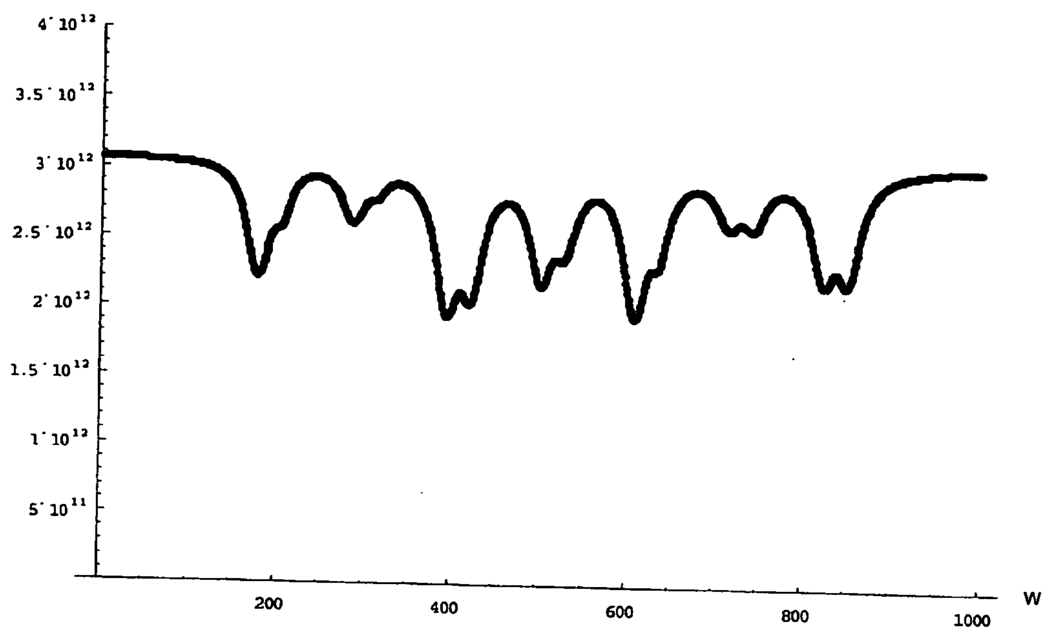

Figure A2. Absorption spectrum for a modulation index of 2.4 but for three different situations regarding absorption coefficient, line width, and Rabi frequency.

Case a: stronger light intensity, $\alpha = 2.1 \times 10^{11}$, $\Gamma = 4 \times 10^{9}$, $\omega_R = 4 \times 10^{6}$, $m = 2.4$

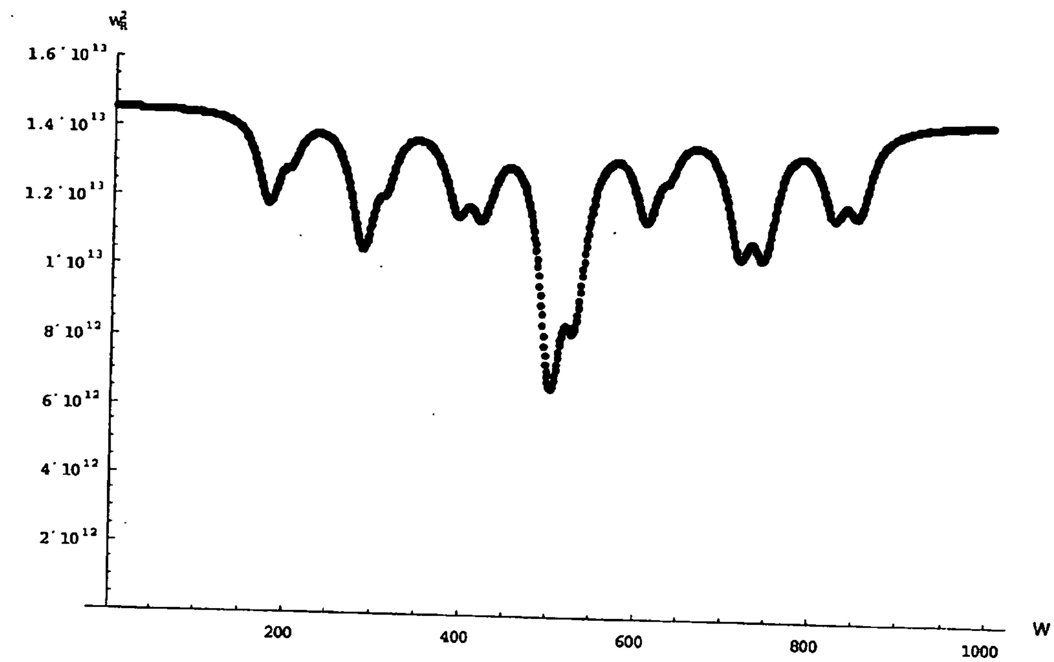

Case b: narrow lines, larger abs. coef., $\alpha = 4.5 \times 10^{11}$, $\Gamma = 2 \times 10^{9}$, $\omega_R = 2 \times 10^{6}$, $m = 2.4$

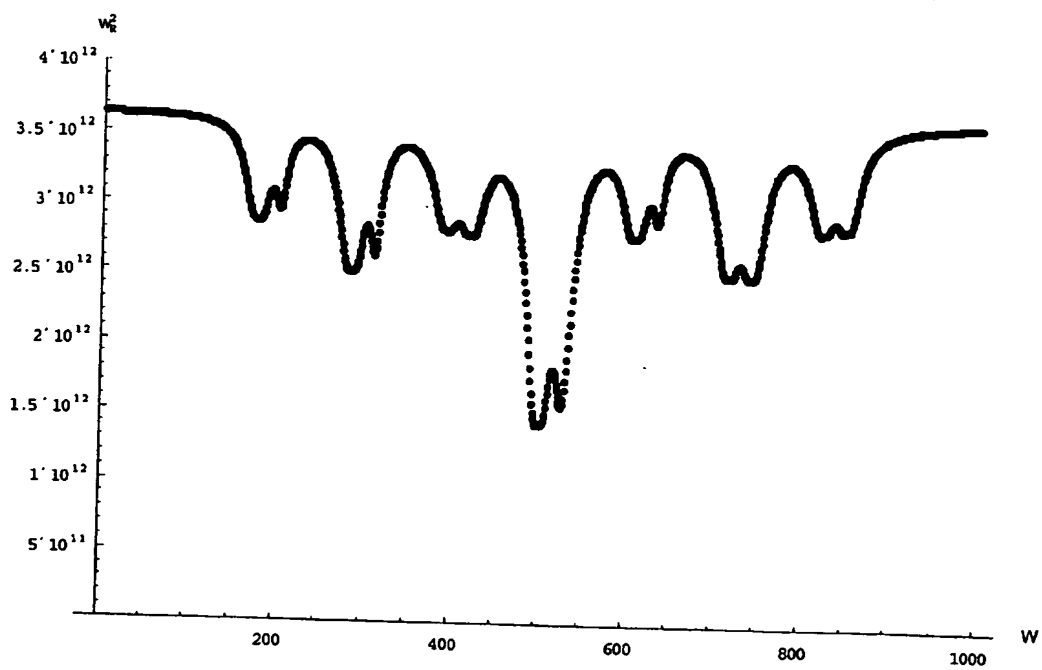

Case c: less absorption but broader line, $\alpha = 1.5 \times 10^{11}$, $\Gamma = 6 \times 10^{9}$, $\omega_R = 2 \times 10^{6}$, m = 2.4

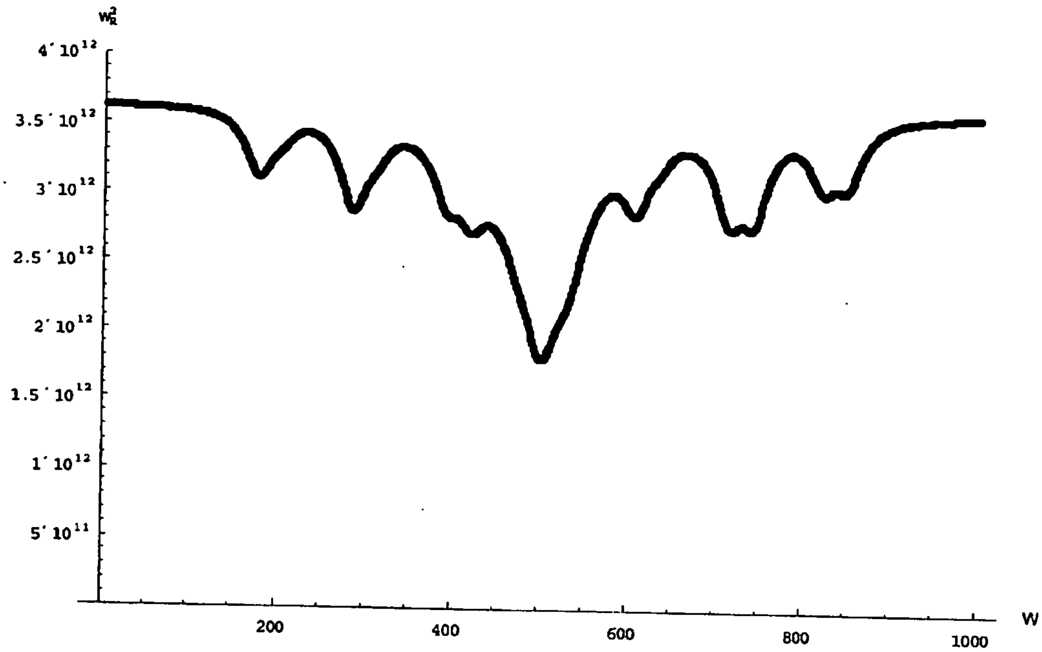

Jacques Vanier
Last edited: Dec. 05, 02

B

IMPLEMENTATION SUPPLEMENT TO:
"On the determination of the laser modulation index from the optical absorption spectrum for clock implementation by CPT" PATENT

The functioning of the coherent population trapping frequency standard, as described in (reference to Vanier patent number) is based on the interaction of a frequency –modulated optical carrier with the hyperfine resonance of an alkali-metal vapor contained within a glass-windowed cell. A typical arrangement is shown in Figure 1 below. The optical carrier is generated by a laser diode which is frequency modulated at one-half the hyperfine resonance frequency of the alkali-metal vapor. For example, for the D1 line of rubidium87 the hyperfine frequency is 6.8 GHz and therefore the laser is modulated at 3.4 GHz.

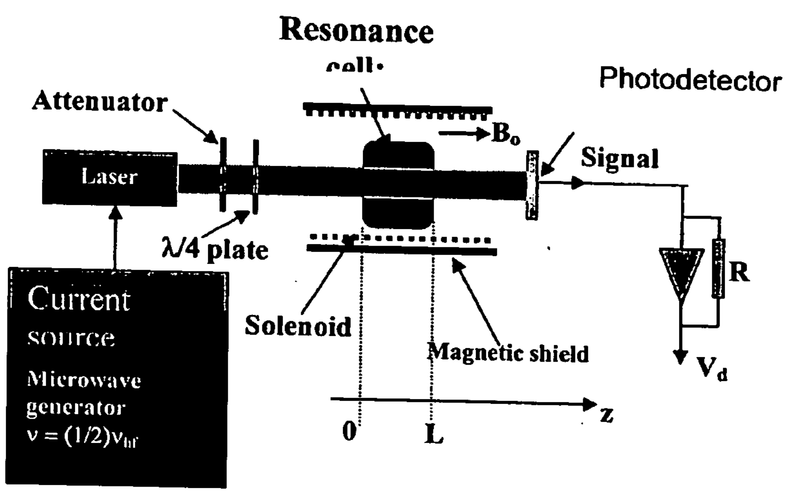

Figure 1 Typical CPT Resonance Configuration

The frequency modulation process generates a set of predictable sidebands disposed symmetrically about the carrier wavelength. The magnitude of these sidebands is shown in Figure 2 as a function of the *modulation index,* which is a measure of the degree of modulation applied to the laser source. It is shown in the references that the performance of a CPT-based frequency standard is critically dependent on the selection and maintenance of specific values of the modulation index. Unfortunately, the experimental determination of the frequency modulation index is difficult and normally requires a specialized optical spectrum analyzer. However, in the special case of the CPT frequency standard schematically shown in Figure 1 it is possible to extract the modulation index from a set of simple measurements and a mathematical algorithm described in the attached reference by Vanier.

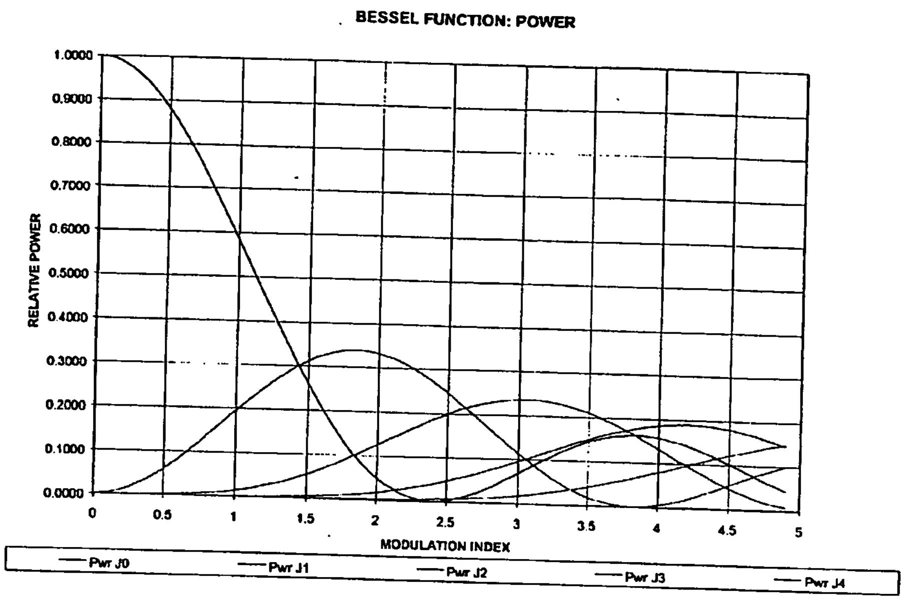

Figure 2: Frequency Modulation Sidebands as a Function of Modulation Index

If the wavelength of an unmodulated laser is slowly swept across the hyperfine resonances of the D1 line of rubidium87, the output of the photodetector of Figure 1 traces out the pattern shown in Figure 3. The resonance features result from transitions from the two hyperfine states of rubidium 87 to the excited state; the vapor becomes essentially opaque at the central wavelength of each transition.

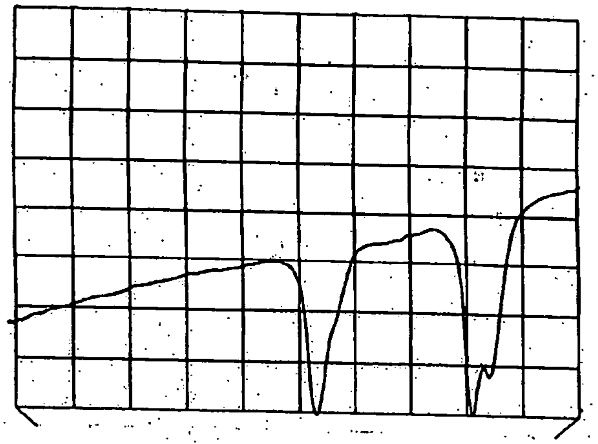

Figure 3: Hyperfine Spectrum of Rubidium87 Using an Unmodulated Laser

However, if the laser source is modulated at approximately one-half the hyperfine separation shown in Figure 3, the resulting spectrum traced out by the photodetector current as the laser wavelength, together with all of the frequency modulation sidebands, is swept over the hyperfine resonances. The spectrum of Figure 4 is mathematically the convolution of the modulated laser spectrum with the hyperfine absorption spectrum: a typical pattern is shown in Figure 4 below.

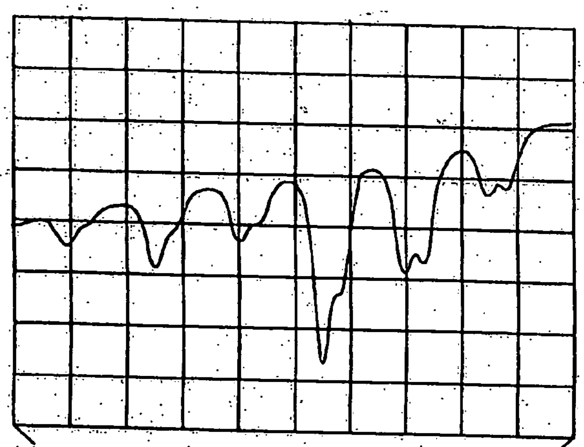

Figure 4: Hyperfine Spectrum of Rubidium87 Using a Frequency Modulated Laser

It is shown in the attached paper by Vanier that Figure 4 expresses all the information required to extract the modulation index of the modulated laser source. The specific procedure can be summarized as follows:

a. The laser source is modulated at approximately one-half the hyperfine separation.
b. The center wavelength of the laser is then slowly swept, by mechanical, thermal or electrical means, through the hyperfine absorption spectrum of the alkali metal vapor.
c. The output current of a photodetector monitoring the optical transmission through the vapor cell is converted to a voltage and digitized by an analog-to-digital converter which

is a component of the frequency standard control servo.

d. The digital values corresponding to each of the minima shown in Figure 4 are passed to a microprocessor, which is a component of the frequency standard control servo.

e. Using the algorithm described in the attached paper by Vanier, the modulation index is determined. The modulation power may then be increased or decreased, as required, produce the desired modulation index.

f. The process is terminated and the functionality of the frequency standard returned to normal operation, as described in the references.

This Page is Inserted by IFW Indexing and Scanning Operations and is not part of the Official Record

BEST AVAILABLE IMAGES

Defective images within this document are accurate representations of the original documents submitted by the applicant.

Defects in the images include but are not limited to the items checked:

- ☑ BLACK BORDERS
- ☐ IMAGE CUT OFF AT TOP, BOTTOM OR SIDES
- ☑ FADED TEXT OR DRAWING
- ☑ BLURRED OR ILLEGIBLE TEXT OR DRAWING
- ☐ SKEWED/SLANTED IMAGES
- ☐ COLOR OR BLACK AND WHITE PHOTOGRAPHS
- ☐ GRAY SCALE DOCUMENTS
- ☐ LINES OR MARKS ON ORIGINAL DOCUMENT
- ☐ REFERENCE(S) OR EXHIBIT(S) SUBMITTED ARE POOR QUALITY
- ☐ OTHER: ______________________

IMAGES ARE BEST AVAILABLE COPY.
As rescanning these documents will not correct the image problems checked, please do not report these problems to the IFW Image Problem Mailbox.